Drynaria rhizome water extract alleviates high-fat diet-induced obesity in mice

TAE-YOUNG GIL[1*], JUNKYU PARK[2*], YEA-JIN PARK[1,3], HYO-JUNG KIM[1], DIVINA C. COMINGUEZ[3] and HYO-JIN AN[1,4]

[1]Department of Oriental Pharmaceutical Science, College of Pharmacy; [2]Department of Science in Korean Medicine, College of Korean Medicine, Graduate School, Kyung Hee University, Seoul 02447; [3]Department of Rehabilitative Medicine of Korean Medicine and Neuropsychiatry, College of Korean Medicine, Sangji University, Wonju, Gangwon 26339; [4]Department of Integrated Drug Development and Natural Products, Graduate School, Kyung Hee University, Seoul 02447, Republic of Korea

Received August 3, 2023; Accepted November 23, 2023

DOI: 10.3892/mmr.2023.13153

Abstract. Drynaria rhizome is a herbal medicine used for strengthening bones and treating bone diseases in East Asia. Although obesity is considered to benefit bone formation, it has been revealed that visceral fat accumulation can promote osteoporosis. Given the complex relationship between bone metabolism and obesity, bone-strengthening medicines should be evaluated while considering the effects of obesity. The present study investigated the effects of Drynaria rhizome extract (DRE) on high-fat diet (HFD)-induced obese mice. DRE was supplemented with the HFD. Body weight, food intake, the expression levels of lipogenesis transcription factors, including sterol regulatory element binding protein (SREBP)-1, peroxisome proliferator-activated receptor (PPAR)-γ and adenosine monophosphate-activated protein kinase (AMPK)-α, and AMPK activation were evaluated. Mice fed DRE and a HFD exhibited reduced body weight without differences in food intake compared with those in the HFD group. Furthermore, DRE; upregulated AMPK-α of epididymal one; down-regulated SREBP-1 and PPAR-γ, as determined using western blotting and quantitative polymerase chain reaction, respectively. Decreased lipid accumulation were observed in both fat pad and liver of HFD-fed mice, which were suppressed by DRE treatment. These results demonstrated the potential of DRE as a dietary natural product for strengthening bones and managing obesity.

Correspondence to: Professor Hyo-Jin An, Department of Oriental Pharmaceutical Science, College of Pharmacy, Kyung Hee University, 26 Kyungheedae-ro, Dongdaemun-gu, Seoul 02447, Republic of Korea
E-mail: hjan@khu.ac.kr

*Contributed equally

Key words: Drynaria rhizome, high-fat diet, sterol regulatory element binding protein-1, peroxisome proliferator-activated receptor-γ, AMP-activated protein kinase

Introduction

Obesity is caused by an imbalance between energy intake and expenditure, resulting in the accumulation of excessive white adipose tissue (WAT) (1). The coronavirus disease 2019 pandemic led to a higher prevalence of obesity, due to restricted outdoor physical activities (2) and unhealthy lifestyle changes (3). Furthermore, obesity predisposes patients with severe acute respiratory syndrome coronavirus-2 infection to severe outcomes (4). The association between obesity, infection and various metabolic diseases including insulin resistance or coronary heart disease is well known (5). Since obesity is caused by immoderate lipid deposition and adipose tissue expansion, inhibiting proliferation and hypertrophy of adipocyte may solve obesity and other metabolic complications (6).

As one of the most complex organs in the human body, adipose tissue consists of lipid-rich cells called adipocytes, which interact with the entire body to maintain metabolic homeostasis (7). Hypertrophy and hyperplasia of the adipose tissue contribute to adipose tissue dysfunction (8). Pathological changes in adipose tissue are reflected by abnormal adipokine secretion, insulin resistance, or prolonged inflammation related to obesity and its associated comorbidities (9). Therefore, understanding the molecular mechanisms underlying adipocyte differentiation, physiology, morphological changes and related factors is necessary to determine the effects of adipocytes. Specifically, adenosine monophosphate-activated protein kinase (AMPK) is an energy sensor that negatively regulates white adipogenesis in the body (10). The AMPK pathway activation inhibits adipocyte proliferation by regulating adipogenic transcription factors, such as sterol regulatory element-binding protein (SREBP)-1 and peroxisome proliferator-activator (PPAR)-γ (10). SREBP-1 is a member of a transcription factor family that regulates lipid homeostasis and metabolism, thereby controlling the synthesis

of endogenous cholesterol, fatty acids, triacylglycerol and phospholipids (11). PPARs are a group of proteins required for fatty acid oxidation and energy metabolism (12). One of the three subtypes of PPARs, PPAR-γ, contributes to energy balance, and lipid and glucose homeostasis regulation as a nuclear receptor superfamily member (13).

Drynaria rhizome is the dried root of *Drynaria fortunei*, a herbaceous perennial plant (14), which has been used to improve bone health by promoting trauma recovery and treating bone fractures (15). As a medicinal herb, the rhizome is classified among the 'Yang-tonifying' or 'kidney-tonifying' herbs specific for bone-related diseases, including osteoporosis or bone fractures, that can regulate bone formation or bone resorption (16-18). Compounds of Drynaria rhizome, such as flavonoids, have exhibited protective effects against osteoarthritis by enhancing bone regeneration (19,20). Since numerous studies have reported on the association between bone health and obesity, it is necessary to investigate therapeutic candidates that can regulate these (21-24). Since obesity may induce an increase in bone density affected by higher mechanical loads or higher 17β-estradiol levels protecting bone (25,26), it seems to be worth to investigate the effects of Drynaria rhizome which is known for bone-related diseases. Previous studies have demonstrated the promoting effects of Drynaria rhizome and its flavonoids on osteoblast differentiation in MC3T3-E1 cells and ovariectomized Sprague-Dawley rats (27-29). Given the increasing evidence of the close relationship between weight loss and bone health (30,31), evaluating the anti-obesity effects of existing reliable medicines for bone disease is important. Therefore, the present study investigated the effects of Drynaria rhizome extract (DRE) supplemented with a high-fat diet (HFD) on HFD-induced obese mice.

Materials and methods

Antibodies. The phosphorylated (p)-AMPK (cat. no. 2535) and AMPK (cat. no. 2532) antibodies were obtained from Cell Signaling Technology, Inc. PPAR-γ (cat. no. sc-7273), SREBP1 (cat. no. sc-13551) and β-actin (cat. no. sc-81178) antibodies were obtained from Santa Cruz Biotechnology, Inc.

Preparation of DRE. The root of the herb *Drynaria fortunei* was purchased from Nanum Pharmaceutical Company (cat. no. HA1800100101). The herb (400 g) was extracted in 4 l hot water at 100˚C for 4 h. The extract was freeze-dried and the yield was calculated at 17.5%; [dried extract weight (38.465 g)/dry starting material weight (219.8 g)] x100 (%).

HFD-induced obese mouse model and treatment. The present study followed the methods of Park *et al* (32). DRE powder was lyophilized, extracted with water at 100˚C for 4 h and purified using filter papers under a vacuum rotary evaporator (EYELA-Tokyo Rikakikai Co., Ltd.); the residual powder was stored at -20˚C until needed. The powder was used to generate a supplemented diet containing 10% DRE and 45% HFD (Research Diets, Inc.); 20 g DRE powder was mixed with 180 of HFD. Male C57BL/6 N mice (specific-pathogen-free grade; age, 8 weeks; weight, 20±2 g) were purchased from Dae Han Bio Link Co., Ltd. The mice were adapted to modified conditions for 1 week, and 30 healthy mice were then used in the present study. The mice were randomly distributed into the following three groups (n=10/group): Normal diet (CON), 45% HFD-induced (HFD), and 45% HFD-induced and 10% DRE-administered (HFD + DRE) groups. The mice were provided *ad libitum* access to food and water. Mice in the HFD + DRE group were provided a HFD for 4 weeks leading to HFD-induced obesity. Subsequently, the mice were fed a HFD supplemented with 10% DRE from week 5. Mice in the CON and HFD groups were fed normal diet and HFD, respectively for 9 weeks. The mice were maintained under a 12/12 h light/dark cycle, at a constant temperature of 22±2˚C and relative humidity of 55±9%. Body weight and food intake were measured weekly. For sacrifice, mice were placed in a 9 l container; 100% of carbon dioxide was supplied to the container at a volume displacement rate of 30% per min (~3 l/min). The flow was continued until 1 min after breathing or heartbeat stopped. Subsequently, cervical dislocation was performed to ensure the animal was sacrificed. All procedures were conducted following the National Institutes of Health guidelines (33) and the present study was approved by the Ethical Committee for Animal Care and the Use of Laboratory Animals of Sangji University (approval no. 2019-11; Wonju, South Korea). At the end of the 10-week period, liver and adipose tissues were obtained, rinsed, weighed and stored at -80˚C until further analysis.

Food efficiency ratio. After sacrifice, body weight gain was divided with food intake. And the value was expressed as percentage).

Weight of eWAT tissues. Relative epididymal white adipose tissues were calculated epididymal WAT weight divided to body weight.

Western blot analysis. Segments of liver or epididymal WAT (eWAT) were suspended in PRO-PREP™ protein extraction solution (Intron Biotechnology, Inc.) and incubated for 20 min at 4˚C. Cell debris was removed via microcentrifugation (20,784 x g, 4˚C for 30 min) followed by quick freezing of the supernatant. Protein concentration was determined using the Bio-Rad protein assay reagent (Bio-Rad Laboratories, Inc.) according to the manufacturer's instructions. Cellular proteins (30 μg) from homogenized adipose tissue were separated by 10-12% SDS-PAGE and electro-blotted onto a polyvinylidene fluoride membrane. The membrane was then incubated for 1 h with blocking solution (5% skim milk) at room temperature, followed by overnight incubation with primary antibodies (1:1,000) at 4˚C. Blots were washed three times with 0.1% Tween 20/Tris-buffered saline (T/TBS) and were then incubated with horseradish peroxidase-conjugated secondary antibodies [Peroxidase AffiniPure Rabbit Anti-Mouse IgG (H+L); cat. no. 315-035-003; Peroxidase AffiniPure Goat Anti-Rabbit IgG (H+L); cat. no. 111-035-003; both from Jackson ImmunoResearch Laboratories Inc. 1:2,500 dilution] for 2 h at room temperature. Blots were again washed three times with T/TBS, and then developed via enhanced chemiluminescence (GE Healthcare). Densitometric analysis

was performed using ImageJ ver 1.53a software (National Institutes of Health).

Reverse-transcription quantitative polymerase chain reaction (RT-qPCR) analysis. Total RNA was extracted from the liver tissue and eWAT using the EASY BLUE RNA extraction kit (iNtRON Biotechnology), according to the manufacturer's instructions. The RNA was then reverse transcribed into cDNA using an Maxime RT PreMix (Random primer, iNtRON Biochnology) according to the manufacturer's protocol. It was conducted using a GeneAmp PCR System 9700 (Applied Biosystems; Thermo Fisher Scientific, Inc.). The synthesized cDNA was 200 bp in size. A StepOnePlus Real-Time PCR System (Applied Biosystems; Thermo Fisher Scientific, Inc.) was used for amplification with Power-SYBR Green PCR Master Mix (Applied Biosystems). The qPCR thermocycling conditions were as follows: Preheating at 92˚C for 2 min, followed by 50 cycles at 92˚C for 30 sec, 60˚C for 30 sec and 68˚C for 30 sec. The expression data were calculated from the quantification cycle (Cq) value using the $2^{-\Delta\Delta Cq}$ method (34). GAPDH was used for normalization. The primer sequences used for RT-qPCR are listed in a previous study (35), as follows: AMPKα, forward (F) 5'-AGAGGGCCGCAATAAAAGAT-3', reverse (R) 5'-TGTTGTACAGGCAGCTGAGG-3'; SREBP1, F 5'-ATCGCAAACAAGCTGACCTG-3', R 5'-AGATCCAGGTTTGAGGTGGG-3'; PPARγ, F 5'-ATCGAGTGCCGAGTCTGTGG-3'; R 5'-GCAAGGCACTTCTGAAACCG-3'; GAPDH, F 5'-GACGGCCGCATCTTCTTGT-3' and R 5'-CACACCGACCTTCACCATTTT-3'.

Biochemical analysis. Briefly, 1.0-1.2 ml total blood was collected from each mouse using cardiac puncture following sacrifice. The collected blood was immediately centrifuged (1,000 x g for 30 min at 4˚C) to obtain plasma. The plasma levels of triglycerides (TG) and total cholesterol (TC) were measured using commercial kits (AM157S-K for TG and AM 202-K for TC) (Asan Pharmaceutical, Co., Ltd.).

Histological analysis. The liver tissue and eWAT from mice in each group were fixed in 10% buffered formalin for 5-10 min for eWAT as well as 20-30 min for liver at 37˚C, embedded in paraffin and cut into 8-μm sections. Sections were stained for 6 h at 60-70˚C with hematoxylin and eosin (H&E) for histological examination of lipid droplets. Adipocyte cell size was determined by measuring 10 randomly selected adipocytes per area of respective tissue and images were acquired using an Olympus SZX10 light stereomicroscope (Olympus Corporation).

Statistical analysis. Data are presented as the mean ± standard deviation of triplicate experiments. The experimental data were analyzed using one-way analysis of variance followed by Dunnett's post hoc test (GraphPad PRISM 5; Dotmatics). $P<0.05$ was considered to indicate a statistically significant difference.

Results

DRE reduces the body weight and serum biochemical parameters of HFD-fed obese mice. Changes in body weight were tracked weekly for 10 weeks. The body weight of the HFD group was significantly increased after 4 weeks compared with that in the CON group (Fig. 1A). DRE was administered via the diet as 10% DRE supplemented in the HFD. The body weight of mice in the HFD + DRE group was lower than that in the HFD group. DRE induced a significant change in body weight at 6 weeks caused by adaptation of mice to the new diet. After 10 weeks, the body weight of mice in the HFD group was significantly increased (35.50±2.76 g) compared with that in the CON group (28.85±0.97 g). In addition, the HFD + DRE group exhibited reduced body weight (31.85±1.95 g) compared with that in the HFD group. Mice were allowed *ad libitum* access to the diet, and food intake was evaluated, showing no differences between the groups (Fig. 1B). To calculate the food efficiency ratio, the equation used to determine the protein efficiency ratio (PER; %) was adapted as follows: Body weight gain (g)/food intake (g) x100 (36). Instead of evaluating the protein quality in food, the present study aimed to assess total food efficiency, which was significantly increased in the HFD group compared to the CON group as well as significantly decreased in the HFD + DRE group comparing to the HFD group (Fig. 1C). At the end of the experiment, after 10 weeks, anatomical examination confirmed the reduced body fat mass in the HFD + DRE group compared with that in the HFD group (Fig. 1D). In addition, after 9 weeks, the levels of serum biochemical markers, TG and TC, were significantly reduced in the HFD + DRE group compared with those in the HFD group and were significantly increased in the HFD group compared with those in the CON group (Fig. 1E and F).

DRE suppresses lipid accumulation in eWAT in HFD-fed obese model mice. Adipose tissue grows via two processes, hypertrophy and hyperplasia (37). In the present study, eWAT exhibited marked changes in size (Fig. 2A) and weight (Fig. 2B). The average weight of eWAT in the HFD group (1.90±0.32 g) was significantly increased compared with that in the CON group (0.70±0.09 g). This increase was suppressed by DRE (1.17±0.32 g) in the HFD + DRE group. This tendency was verified by determining relative eWAT weight (tissue weight/body weight) (Fig. 2C). To determine the effects of DRE on adipose tissue growth and lipid accumulation, H&E staining was performed on eWAT (Fig. 2D). As shown in Fig. 2D and E, the HFD group exhibited an increase in adipocyte size (113.22±4.57 μm) compared with that in the CON group (63.86±6.30 μm); however, mice in the HFD + DRE group exhibited decreased adipocyte diameter (81.93±3.61 μm) compared with that in the HFD group.

DRE downregulates the expression of adipogenic markers in the eWAT of HFD-induced obese mice. Western blotting was conducted to clarify the effect of DRE on the expression levels of adipogenic transcription factors in eWAT. The HFD + DRE group exhibited restored protein expression of p-AMPK-α compared with that in the HFD group, which was significantly decreased compared with the CON group (Fig. 3A and B). Given the regulatory effect of DRE on p-AMPK-α (Fig. 3A and B), the protein expression levels of adipogenic transcription factors, SREBP-1 and PPAR-γ, were determined. The increased protein expression levels induced by

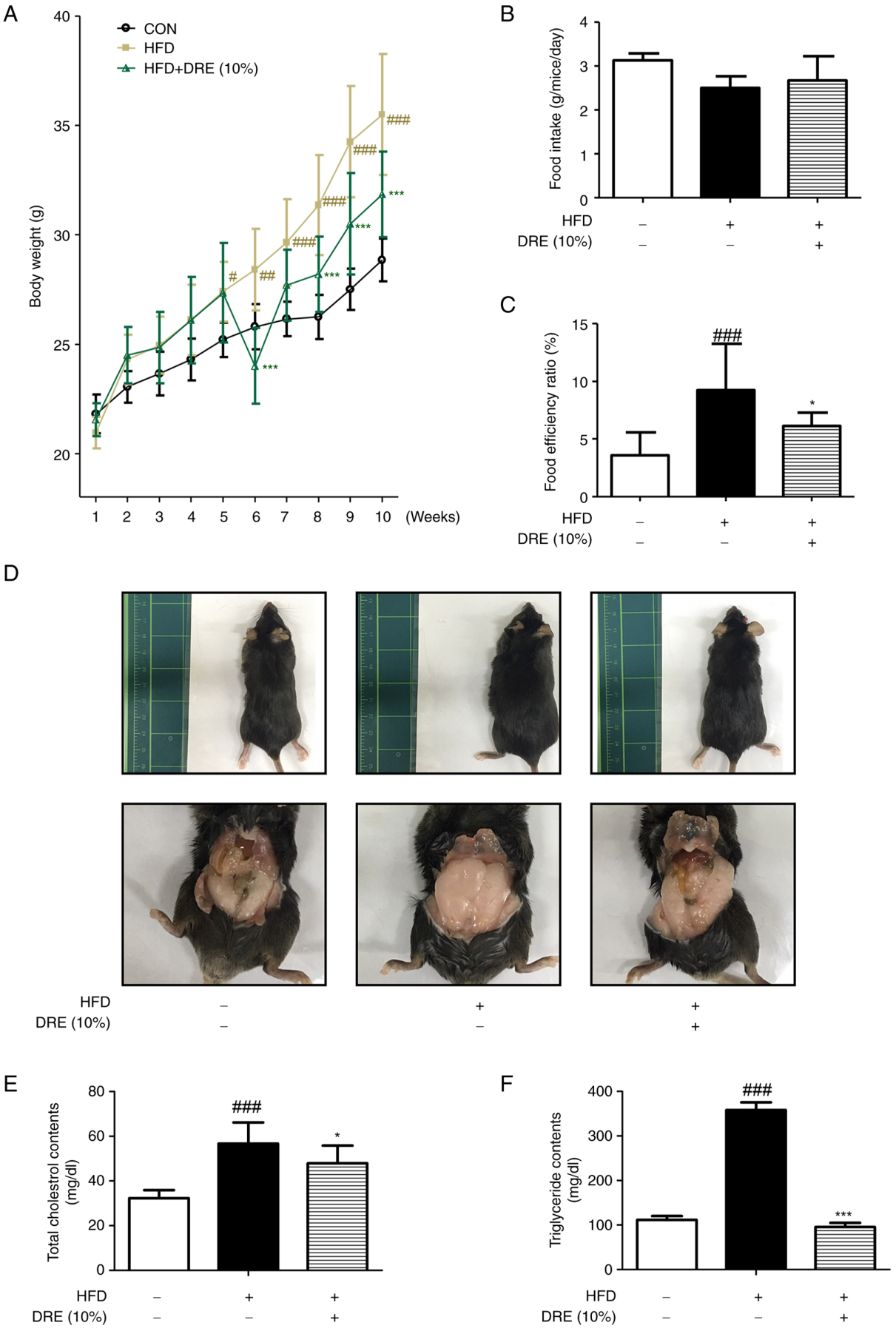

Figure 1. Effects of DRE on body weight and food intake in HFD-induced obese mice. (A) Mouse body weight was measured weekly for 10 weeks and (B) food intake was calculated as g/mouse/day. (C) Food efficiency ratio was calculated. (D) Images of mouse bodies and the abdominal cavity. Serum biochemical parameters (E) total cholesterol and (F) triglyceride were examined. Data are presented as the mean ± standard deviation. $^{\#}$P<0.05, $^{\#\#}$P<0.01 and $^{\#\#\#}$P<0.001 vs. CON group; *P<0.05 and ***P<0.001 vs. HFD group. CON, control; DRE, Drynaria rhizome extract; HFD, high-fat diet.

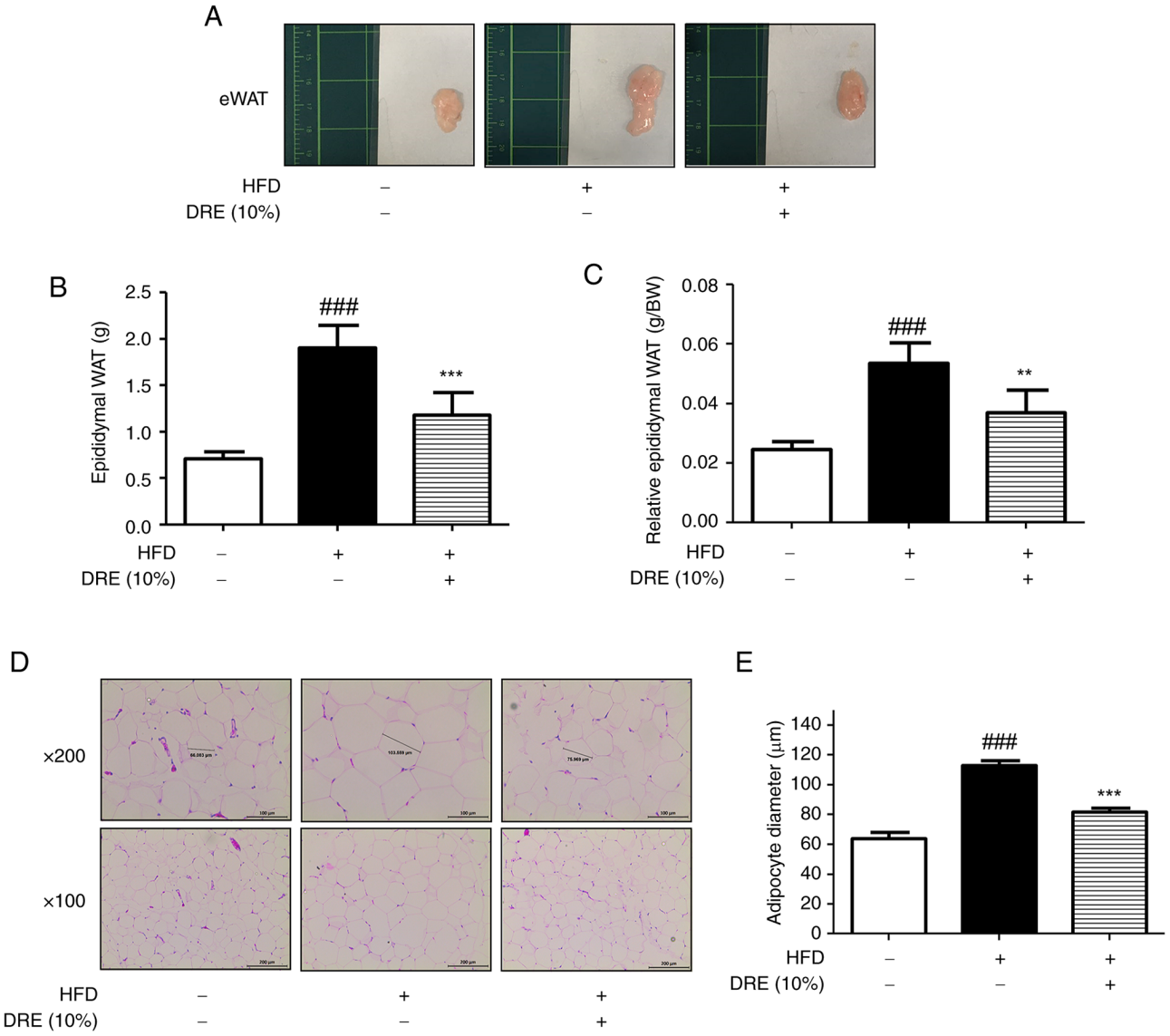

Figure 2. Effect of DRE on eWAT expansion in HFD-induced obese mice. (A) Representative eWAT images, (B) average tissue weight and (C) relative tissue weight after 10 weeks of the experiment. Representative images of eWAT stained with (D) hematoxylin and eosin, and (E) average adipocyte diameter in the tissue. Data are presented as the mean ± standard deviation. $^{###}$P<0.001 vs. control group; **P<0.01 and ***P<0.001 vs. HFD group. BW, body weight; DRE, Drynaria rhizome extract; eWAT, epididymal white adipose tissue; HFD, high-fat diet.

HFD were mitigated by DRE dietary treatment (Fig. 3C-E). To assess the mRNA expression levels of these factors, RT-qPCR analysis was performed. The mRNA expression levels were consistent with the protein expression levels. DRE upregulated AMPK activation, and a downregulatory effect on SREBP-1 or PPAR-γ expression (Fig. 3F).

DRE ameliorates lipid accumulation in the liver of HFD-fed obese model mice. Excessive fat accumulation in the liver leads to fatty liver diseases, such as nonalcoholic fatty liver disease (38). Therefore, the present study observed the size and color of liver tissue and compared its weight between groups. Bigger liver tissue of HFD group compared to CON group was presented and brighter liver tissue of HFD + DRE group comparing to CON or HFD group was shown (Fig. 4A), there was no statistically significant difference in liver weight among the three groups (Fig. 4B). However, histological examination with H&E confirmed that HFD-induced lipid accumulation was alleviated by DRE, resulting in smaller and less frequent lipid droplets, as indicated with black arrows (Fig. 4C).

DRE suppresses adipogenic marker expression in the liver in HFD-induced obese mice. The present study assessed the mRNA and protein expression levels of adipogenesis factors via RT-qPCR and western blot analysis, respectively. Unlike the changes in AMPK activation observed in eWAT and protein expression of liver, the difference in the mRNA expression levels of AMPK among the groups was not significant (Fig. 5A, B and F). Also, DRE treatment didn't significantly recover the protein expression of AMPK phosphorylation comparing to HFD group whereas apparently decreased phosphorylated AMPK expression in HFD group. However, the adipogenic transcription factor SREBP-1, and its direct target PPAR-γ, were markedly induced by HFD and suppressed by DRE dietary treatment (Fig. 5C-F). In Fig. 5B, D, and E, the relative density of protein expression was presented.

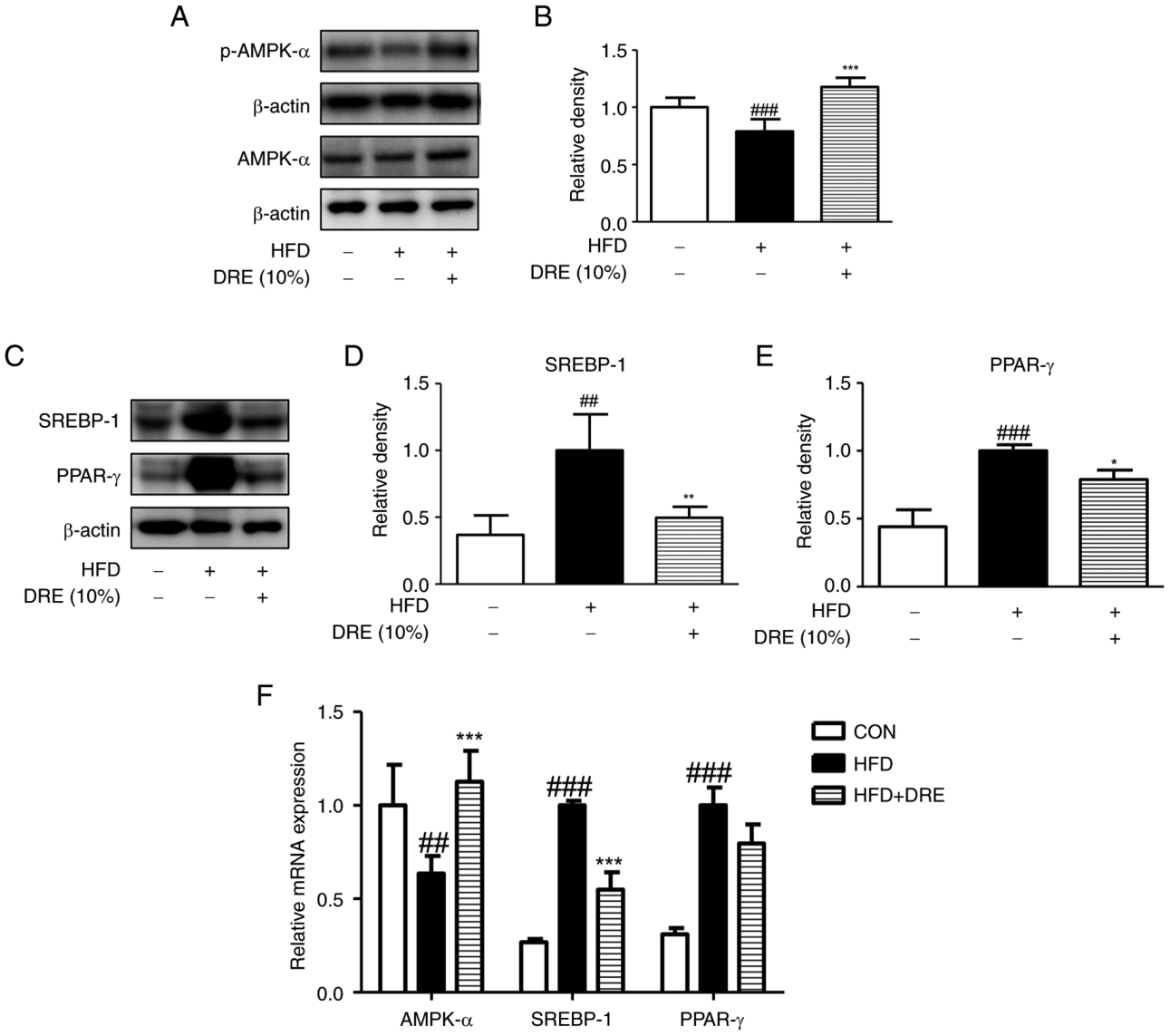

Figure 3. Effect of DRE on the expression levels of adipogenic transcription factors in the eWAT of HFD-induced obese mice. (A) Representative western blot and (B) semi-quantification of p-AMPK-α protein expression levels in eWAT. P-AMPK expression was normalized to AMPK using ImageJ v1.50i. (C) Representative western blot, and semi-quantification of (D) SREBP-1 and (E) PPAR-γ protein expression levels in eWAT. Expression was normalized to β-actin using ImageJ v1.50i. (F) AMPK-α, SREBP-1 and PPAR-γ mRNA expression levels were detected in eWAT using reverse transcription-quantitative polymerase chain reaction. Relative mRNA expression levels were normalized to GAPDH. Data are presented as the mean ± standard deviation. $^{\#\#}$P<0.01 and $^{\#\#\#}$P<0.001 vs. CON group; *P<0.05, **P<0.01 and ***P<0.001 vs. HFD group. AMPK-α, adenosine monophosphate-activated protein kinase-α; CON, control; DRE, Drynaria rhizome extract; eWAT, epididymal white adipose tissue; HFD, high-fat diet; p-, phosphorylated; PPAR-γ, peroxisome proliferator-activated receptor-γ; SREBP-1, sterol regulatory element binding protein-1.

Discussion

In drug development, interest in drug repurposing has increased, with the aim of uncovering novel therapeutic indications of proven drugs (39). Drynaria rhizome has been used for bone health and blood revitalization, and is mainly prescribed for bone formation or fractures due to its warm (nature) and bitter taste (40-43). The compounds of Drynaria rhizome have been suggested to treat osteoporosis (44). In addition, it is known that Drynaria rhizome has no obvious toxic side effects (41). Drynaria rhizome contains various bioactive compounds with the capacity for alleviating obesity, such as (-)-epicatechin or narigin (45,46). Recent studies have focused on the complex relationship between bone health and obesity, including the effect of adipokines on bone cells and bone metabolism in type 2 diabetes (22,26,47). Therefore, the present study evaluated the effects of the root of *D. fortunei* on obesity.

A HFD is the primary promotor of obesity by inducing an imbalance in energy expenditure and intake (48). Therefore, the HFD-induced obesity mouse model is a well-established *in vivo* experimental model for research on obesity (49). The present study used a 45% HFD-induced obese C57BL/6 mouse model. To mimic the influence of food and minimize stress in mice, the experimental preparation (DRE) was mixed with the HFD at a concentration of 10%. The dosage and method of DRE administration were selected according to the recommendations of previous studies (35,50,51). Body weight was measured weekly and obesity was revealed to be significantly induced after 5 weeks. Differential weight loss by

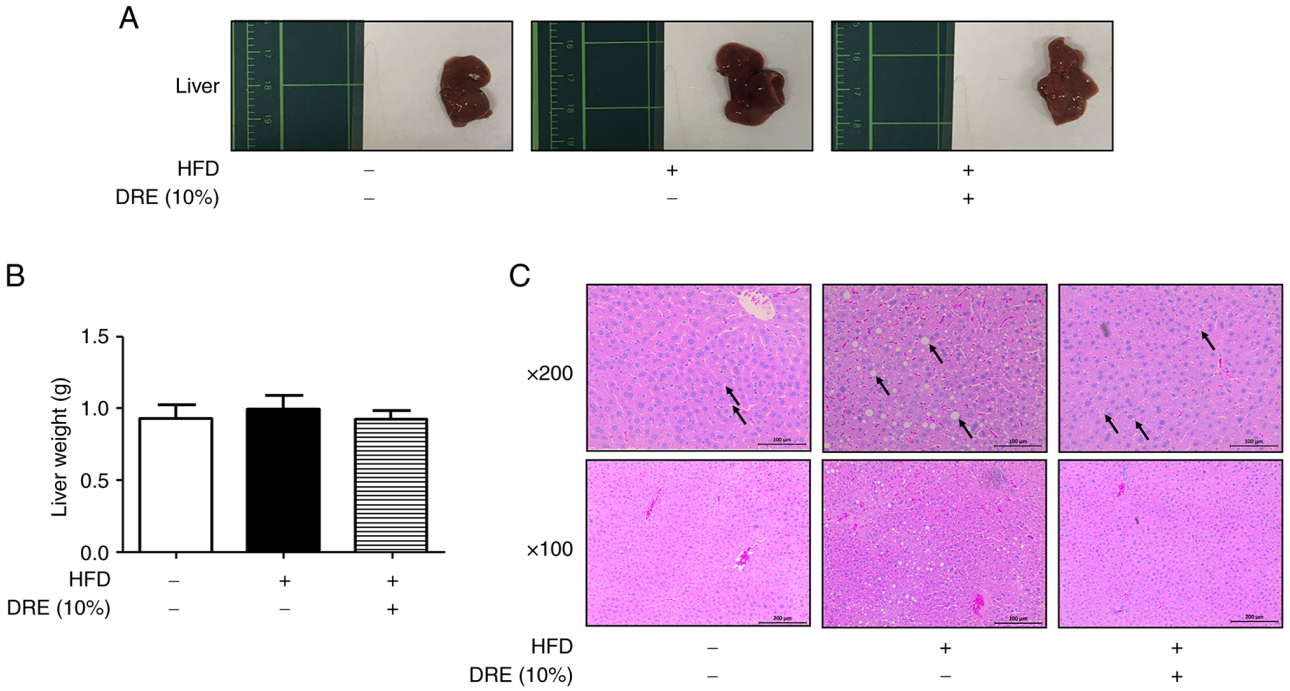

Figure 4. Effect of DRE on the changes in liver tissue in HFD-induced obese mice. (A) Representative images of liver tissue and (B) average liver tissue weight. (C) Images of hematoxylin and eosin-stained liver tissue. Black arrows indicate lipid droplets. DRE, Drynaria rhizome extract; HFD, high-fat diet.

DRE after 8 weeks of the administration. Despite similar food intake across the groups, obesity was significantly alleviated in the DRE-supplemented group. Nutritional factors affected by DRE were determined by modified PER, which represents the weight gain of a subject divided by the intake of dietary protein during the experimental period (52). Furthermore, it seems to be valuable to determine the effects of DRE on the efficiency of food digestion and absorption to evaluation intestinal capacity for further study. The increased body fat mass was determined based on the appearance of eWAT in the abdominal cavity.

As the abnormal expansion and accumulation of eWAT are considered characteristics of obesity, the present study investigated the histological and molecular changes in eWAT (53). A HFD induced a significant increase in the weight and size of eWAT, which indicated adipocyte expansion and hyperplasia. These morphological changes were histologically confirmed under a microscope via H&E staining indicating lipid accumulation (54,55). Additionally, DRE alleviated the increase in adipocyte diameter induced by HFD. Furthermore the protein and mRNA expression levels of lipogenesis-related markers, AMPK, SREBP-1 and PPAR-γ, were altered by DRE dietary supplementation. AMPK is a protein kinase involved in metabolism, which regulates adipogenic transcription factors, including SREBP-1 and PPAR-γ (56), and suppresses insulin resistance (57). Furthermore, it has been reported that total flavonoids of Drynaria rhizome exhibit efficacy in treating osteoarthritis via the AMPK/NF-κB pathway (58). In the present study, DRE upregulated p-AMPK expression under HFD-induced obesity conditions. AMPK and its downstream proteins maintain energy homeostasis in adipose tissues (59). The effects of DRE on the molecular level of AMPK-α, SREBP-1, or PPAR-γ were assessed using western blotting and RT-qPCR. DRE treatment induced up-regulated protein and mRNA expression of AMPK-α comparing to the ones in HFD group. Also, SREBP-1 and PPAR-γR were showed suppressed protein and mRNA expression by DRE treatment comparing to the ones in HFD group.

The effects of DRE were also notable on liver tissue. Even though the differences in weight and AMPK phosphorylation in the liver were not significant among the groups, the activation and expression of adipogenic transcription factors were suppressed in the DRE-supplemented group compared with that in the HFD group. Since AMPK is considered to improve lipid metabolic disorders by inhibiting SREBP activity, the present study expected to observe a recovery effect of DRE on the decreased p-AMPK expression in the eWAT from HFD-induced obese mice (60). However, the mRNA expression of AMPK exhibited no significant changes among the groups in the liver, unlike those detected in eWAT. This may be due to the involvement of other molecular biomarkers, or differences among the tissues, liver and eWAT, such as CCAAT/enhancer-binding protein or other subunits of AMPK, including AMPK-β or AMPK-γ (61,62). To identify the exact signaling pathways in the future, it is necessary to perform *in vitro* studies on the effects of DRE on preadipocytes, their differentiation and other adipogenic transcription factors. In addition, it is necessary to investigate the association between the molecular mechanisms and different tissues for further study such as fatty liver diseases (61).

In conclusion, despite limited data on the mechanism, the present study demonstrated through an *in vivo* model that DRE exerts its effects on HFD-induced obesity by downregulating related transcription factors (Fig. 6), providing insight into the potential role of herbal medicines in alleviating both obesity and improving bone health.

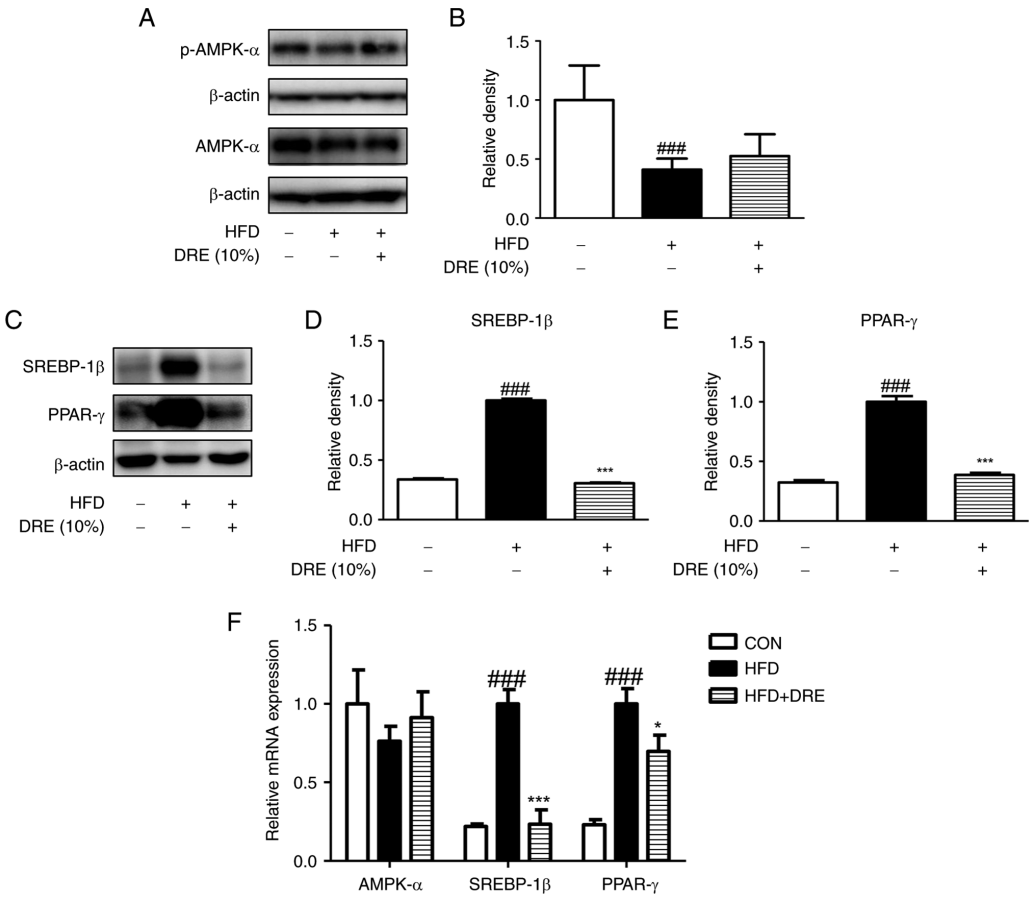

Figure 5. Effect of DRE on adipogenesis in the liver in HFD-induced obese mice. (A) Representative western blot and (B) semi-quantification of p-AMPK-α protein expression levels in liver tissue. P-AMPK expression was normalized to AMPK using ImageJ v1.50i. (C) Representative western blot, and semi-quantification of (D) SREBP-1 and (E) PPAR-γ protein expression levels in liver tissue. Expression was normalized to β-actin using ImageJ v1.50i. (F) AMPK-α, SREBP-1 and PPAR-γ mRNA expression levels in the liver were determined using reverse transcription-quantitative polymerase chain reaction. Relative mRNA expression levels were normalized to GAPDH. Data are presented as the mean ± standard deviation. $^{###}$P<0.001 vs. CON group; *P<0.05 and ***P<0.001 vs. HFD group. AMPK-α, adenosine monophosphate-activated protein kinase-α; CON, control; DRE, Drynaria rhizome extract; eWAT, epididymal white adipose tissue; HFD, high-fat diet; p-, phosphorylated; PPAR-γ, peroxisome proliferator-activated receptor-γ; SREBP-1, sterol regulatory element binding protein-1.

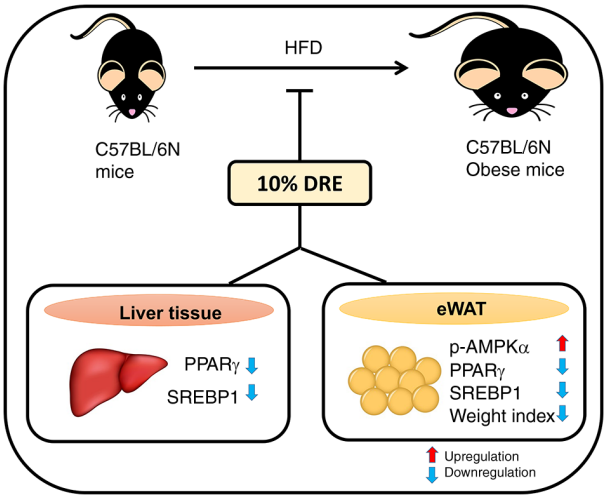

Figure 6. Mechanism underlying DRE activity in HFD-induced obese model mice. DRE dietary administration reduced the expression of the adipogenic transcription factors SREBP-1 and PPAR-γ in the liver and eWAT by regulating the AMPK pathway. AMPK-α, adenosine monophosphate-activated protein kinase-α; DRE, Drynaria rhizome extract; eWAT, epididymal white adipose tissue; HFD, high-fat diet; p-, phosphorylated; PPAR-γ, peroxisome proliferator-activated receptor-γ; SREBP-1, sterol regulatory element binding protein-1.

Acknowledgements

Not applicable.

Funding

This research was supported by a National Research Foundation of Korea (NRF) grant funded by the Korea Government Ministry of Science and ICT (grant no. NRF-2021R1A2C3011862).

Availability of data and materials

The datasets used and/or analyzed during the current study are available from the corresponding author on reasonable request.

Authors' contributions

TYG, JP and HJA conceived and designed the experiments. YJP, HYK and DCC performed the experiments. TYG and JP analyzed the data. HJA contributed reagents, materials and

analysis tools, and was involved in revisiting the manuscript critically for crucial intellectual contents. TYG and HJA wrote the paper. HJA and TYG confirm the authenticity of all the raw data. All authors read and approved the final manuscript.

Ethics approval and consent to participate

All procedures followed the National Institute of Health guidelines and the present study was approved by the Ethical Committee for Animal Care and the Use of Laboratory Animals of Sangji University (approval no. 2019-11).

Patient consent for publication

Not applicable.

Competing interests

The authors declare that they have no competing interests.

References

1. Hall KD, Farooqi IS, Friedman JM, Klein S, Loos RJF, Mangelsdorf DJ, O'Rahilly S, Ravussin E, Redman LM, Ryan DH, *et al*: The energy balance model of obesity: Beyond calories in, calories out. Am J Clin Nutr 115: 1243-1254, 2022.
2. Michelini E, Bortoletto N and Porrovecchio A: Outdoor physical activity during the first wave of the COVID-19 Pandemic. A comparative analysis of Government Restrictions in Italy, France, and Germany. Front Public Health 9: 615745, 2021.
3. Holly JMP, Biernacka K, Maskell N and Perks CM: Obesity, Diabetes and COVID-19: an infectious disease spreading from the East Collides With the Consequences of an Unhealthy Western Lifestyle. Front Endocrinol (Lausanne) 11: 582870, 2020.
4. Sattar N, McInnes IB and McMurray JJV: Obesity is a risk factor for severe COVID-19 Infection: Multiple potential mechanisms. Circulation 142: 4-6, 2020.
5. Engin A: The definition and prevalence of obesity and metabolic syndrome. Adv Exp Med Biol 960: 1-17, 2017.
6. Longo M, Zatterale F, Naderi J, Parrillo L, Formisano P, Raciti GA, Beguinot F and Miele C: Adipose tissue dysfunction as determinant of obesity-associated metabolic complications. Int J Mol Sci 20: 2358, 2019.
7. Choe SS, Huh JY, Hwang IJ, Kim JI and Kim JB: Adipose tissue remodeling: Its role in energy metabolism and metabolic disorders. Front Endocrinol (Lausanne) 7: 30, 2016.
8. Spiegelman BM and Flier JS: Obesity and the regulation of energy balance. Cell 104: 531-543, 2001.
9. van Tienen FH, Laeremans H, van der Kallen CJ and Smeets HJ: Wnt5b stimulates adipogenesis by activating PPARgamma, and inhibiting the beta-catenin dependent Wnt signaling pathway together with Wnt5a. Biochem Biophys Res Commun 387: 207-211, 2009.
10. Ahmad B, Serpell CJ, Fong IL and Wong EH: Molecular mechanisms of adipogenesis: The Anti-adipogenic Role of AMP-Activated protein kinase. Front Mol Biosci 7: 76, 2020.
11. Eberle D, Hegarty B, Bossard P, Ferre P and Foufelle F: SREBP transcription factors: Master regulators of lipid homeostasis. Biochimie 86: 839-848, 2004.
12. Hernandez-Quiles M, Broekema MF and Kalkhoven E: PPARgamma in metabolism, immunity, and cancer: Unified and diverse mechanisms of action. Front Endocrinol (Lausanne) 12: 624112, 2021.
13. Wang QA, Zhang F, Jiang L, Ye R, An Y, Shao M, Tao C, Gupta RK and Scherer PE: Peroxisome proliferator-activated receptor gamma and its role in adipocyte homeostasis and thiazolidinedione-mediated insulin sensitization. Mol Cell Biol 38: e00677-17, 2018.
14. Ettinger B, Genant HK and Cann CE: Postmenopausal bone loss is prevented by treatment with low-dosage estrogen with calcium. Ann Intern Med 106: 40-45, 1987.
15. Zhu YP: Chinese Materia Medica: Chemistry, Pharmacology and Applications. CRC Press, Boca Raton, FL, USA, pp 593-609 1998.
16. Zhou L, Wong KY, Poon CC, Yu W, Xiao H, Chan CO, Mok DK and Wong MS: Water extract of rhizoma drynaria selectively exerts estrogenic activities in ovariectomized rats and estrogen receptor-positive cells. Front Endocrinol (Lausanne) 13: 817146, 2022.
17. Wong RW and Rabie AB: Systemic effect of crude extract from rhizome of Drynaria fortunei on bone formation in mice. Phytother Res 20: 313-315, 2006.
18. Chen LL, Lei LH, Ding PH, Tang Q and Wu YM: Osteogenic effect of Drynariae rhizoma extracts and Naringin on MC3T3-E1 cells and an induced rat alveolar bone resorption model. Arch Oral Biol 56: 1655-1662, 2011.
19. Zhao Y, Cai X, Sun J, Bi W and Yu Y: Active components and mechanisms of total flavonoids from Rhizoma Drynariae in enhancing cranial bone regeneration: An investigation employing serum pharmacochemistry and network pharmacology approaches. J Ethnopharmacol 319(Pt 3): 117253, 2024.
20. Song S, Gao Z, Lei X, Niu Y, Zhang Y, Li C, Lu Y, Wang Z and Shang P: Total Flavonoids of drynariae rhizoma prevent bone loss induced by hindlimb unloading in rats. Molecules 22: 1033, 2017.
21. Rinonapoli G, Pace V, Ruggiero C, Ceccarini P, Bisaccia M, Meccariello L and Caraffa A: Obesity and Bone: A Complex Relationship. Int J Mol Sci 22: 13662, 2021.
22. Zhao P, Xu A and Leung WK: Obesity, bone loss, and periodontitis: The Interlink. Biomolecules 12: 865, 2022.
23. Gkastaris K, Goulis DG, Potoupnis M, Anastasilakis AD and Kapetanos G: Obesity, osteoporosis and bone metabolism. J Musculoskelet Neuronal Interact 20: 372-381, 2020.
24. Pedersen BK and Febbraio MA: Muscles, exercise and obesity: Skeletal muscle as a secretory organ. Nat Rev Endocrinol 8: 457-465, 2012.
25. Qiao D, Li Y, Liu X, Zhang X, Qian X, Zhang H, Zhang G and Wang C: Association of obesity with bone mineral density and osteoporosis in adults: A systematic review and meta-analysis. Public Health 180: 22-28, 2020.
26. Hou J, He C, He W, Yang M, Luo X and Li C: Obesity and bone health: A complex link. Front Cell Dev Biol 8: 600181, 2020.
27. Hu Y, Mu P, Ma X, Shi J, Zhong Z and Huang L: Rhizoma drynariae total flavonoids combined with calcium carbonate ameliorates bone loss in experimentally induced Osteoporosis in rats via the regulation of Wnt3a/β-catenin pathway. J Orthop Surg Res 16: 702, 2021.
28. Li S, Zhou H, Hu C, Yang J, Ye J, Zhou Y, Li Z, Chen L and Zhou Q: Total Flavonoids of Rhizoma drynariae promotes differentiation of osteoblasts and growth of bone graft in induced membrane partly by activating wnt/β-catenin signaling pathway. Front Pharmacol 12: 675470, 2021.
29. Jeong JC, Lee JW, Yoon CH, Kim HM and Kim CH: Drynariae Rhizoma promotes osteoblast differentiation and mineralization in MC3T3-E1 cells through regulation of bone morphogenetic protein-2, alkaline phosphatase, type I collagen and collagenase-1. Toxicol In Vitro 18: 829-834, 2004.
30. Zhang Y, Tan C and Tan W: BMI, socioeconomic status, and bone mineral density in U.S. adults: Mediation analysis in the NHANES. Front Nutr 10: 1132234, 2023.
31. Pinar-Gutierrez A, Garcia-Fontana C, Garcia-Fontana B and Munoz-Torres M: Obesity and bone health: A complex relationship. Int J Mol Sci 23: 8303, 2022.
32. Park YJ, Lee GS, Cheon SY, Cha YY and An HJ: The anti-obesity effects of Tongbi-san in a high-fat diet-induced obese mouse model. BMC Complement Altern Med 19: 1, 2019.
33. Institute of Laboratory Animal Resources (US) and the Committee on Care, and Use of Laboratory Animals: Guide for the Care and Use of Laboratory Animals. US Department of Health and Human Services, Public Health Service, National Institutes of Health, Bethseda, MD, USA, pp 46-68, 1986.
34. Rao X, Huang X, Zhou Z and Lin X: An improvement of the 2^(-delta delta CT) method for quantitative real-time polymerase chain reaction data analysis. Biostat Bioinforma Biomath 3: 71-85, 2013.
35. Park YJ, Seo DW, Gil TY, Cominguez DC, Lee H, Lee DS, Han I and An HJ: Pharmacological Properties of a Traditional Korean Formula Bojungchiseup-tang on 3T3-L1 preadipocytes and high-fat diet-induced obesity mouse model. Biomed Res Int 2020: 8851010, 2020.
36. Balogun JK, Auta J, Abdullahi SA and Agboola OE: Potentials of castor seed meal (*Ricinus communis L.)* as feed ingredient for Oreochromis niloticus. Proceedings of the 19th Annual Conference of the Fisheries Society of Nigeria (FISON): Ilorin, 29th November-3rd December, 2004. Fisheries Society of Nigeria Publications: 838-843, 2005.

37. Ciesielska K and Gajewska M: Fatty acids as potent modulators of autophagy activity in white adipose tissue. Biomolecules 13: 255, 2023.
38. Geisler CE and Renquist BJ: Hepatic lipid accumulation: Cause and consequence of dysregulated glucoregulatory hormones. J Endocrinol 234: R1-R21, 2017.
39. Krishnamurthy N, Grimshaw AA, Axson SA, Choe SH and Miller JE: Drug repurposing: A systematic review on root causes, barriers and facilitators. BMC Health Serv Res 22: 970, 2022.
40. Jeong JC, Lee BT, Yoon CH, Kim HM and Kim CH: Effects of Drynariae rhizoma on the proliferation of human bone cells and the immunomodulatory activity. Pharmacol Res 51: 125-136, 2005.
41. Chen SQ, Liang W, Zhang XM, Li X, Zhan ZL, Guo LP, Huang LQ, Zhang XM and Gao WY: Research progress on chemical compositions and pharmacological action of Drynariae Rhizoma. Zhongguo Zhong Yao Za Zhi 46: 2737-2745, 2021 (In Chinese).
42. Wong RW and Rabie AB: Traditional Chinese medicines and bone formation-a review. J Oral Maxillofac Surg 64: 828-837, 2006.
43. Wong RW, Rabie B, Bendeus M and Hagg U: The effects of rhizoma curculiginis and rhizoma drynariae extracts on bones. Chin Med 2: 13, 2007.
44. Zhang Y, Jiang J, Shen H, Chai Y, Wei X and Xie Y: Total flavonoids from Rhizoma Drynariae (Gusuibu) for treating osteoporotic fractures: implication in clinical practice. Drug Des Devel Ther 11: 1881-1890, 2017.
45. Bettaieb A, Cremonini E, Kang H, Kang J, Haj FG and Oteiza PI: Anti-inflammatory actions of (-)-epicatechin in the adipose tissue of obese mice. Int J Biochem Cell Biol 81(Pt B): 383-392, 2016.
46. Lee HS, Heo CU, Song YH, Lee K and Choi CI: Naringin promotes fat browning mediated by UCP1 activation via the AMPK signaling pathway in 3T3-L1 adipocytes. Arch Pharm Res 46: 192-205, 2023.
47. Kirk B, Feehan J, Lombardi G and Duque G: Muscle, bone, and fat crosstalk: The biological role of myokines, osteokines, and adipokines. Curr Osteoporos Rep 18: 388-400, 2020.
48. Romieu I, Dossus L, Barquera S, Blottière HM, Franks PW, Gunter M, Hwalla N, Hursting SD, Leitzmann M, Margetts B, *et al*: Energy balance and obesity: what are the main drivers? Cancer Causes Control 28: 247-258, 2017.
49. de Moura E Dias M, Dos Reis SA, da Conceicao LL, Sediyama CMNO, Pereira SS, de Oliveira LL, Gouveia Peluzio MDC, Martinez JA and Milagro FI: Diet-induced obesity in animal models: Points to consider and influence on metabolic markers. Diabetol Metab Syndr 13: 32, 2021.
50. An HJ, Rim HK, Suh SE, Jeong HJ, Um JY, Hong SH and Kim HM: Gamiwalbitang, composed of four herbs, controls body weight increase and lipid level elevation induced by a high-fat diet in mice. Immunopharmacol Immunotoxicol 32: 307-312, 2010.
51. An HJ, Chung HS, Kim NH, Hong SH, Park EJ, Baek SH and Kim HM: Regulatory effect of sense line diet on cholesterol and body weight in mice fed a high-fat diet. Ann Nutr Metab 48: 398-403, 2004.
52. Funk MD, Lee M, Vidoni ML and Reininger BM: Weight loss and weight gain among participants in a community-based weight loss Challenge. BMC Obes 6: 2, 2019.
53. Wang X, Zhao Y, Zhou D, Tian Y, Feng G and Lu Z: Gab2 deficiency suppresses high-fat diet-induced obesity by reducing adipose tissue inflammation and increasing brown adipose function in mice. Cell Death Dis 12: 212, 2021.
54. Lizardo K, Ayyappan JP, Oswal N, Weiss LM, Scherer PE and Nagajyothi JF: Fat tissue regulates the pathogenesis and severity of cardiomyopathy in murine chagas disease. PLoS Negl Trop Dis 15: e0008964, 2021.
55. Cui A, Hu Z, Han Y, Yang Y and Li Y: Optimized analysis of in vivo and in vitro hepatic steatosis. J Vis Exp (121):55178, 2017.
56. Canto C and Auwerx J: PGC-1alpha, SIRT1 and AMPK, an energy sensing network that controls energy expenditure. Curr Opin Lipidol 20: 98-105, 2009.
57. Garcia D, Hellberg K, Chaix A, Wallace M, Herzig S, Badur MG, Lin T, Shokhirev MN, Pinto AFM, Ross DS, *et al*: Genetic Liver-Specific AMPK activation protects against diet-induced obesity and NAFLD. Cell Rep 26: 192-208 e6, 2019.
58. Chen GY, Liu XY, Yan XE, Yu X, Liu Y, Luo J and Tao QW: Total flavonoids of rhizoma drynariae treat osteoarthritis by inhibiting arachidonic acid metabolites through AMPK/NFκB pathway. J Inflamm Res 16: 4123-4140, 2023.
59. Ix JH and Sharma K: Mechanisms linking obesity, chronic kidney disease, and fatty liver disease: The roles of fetuin-A, adiponectin, and AMPK. J Am Soc Nephrol 21: 406-412, 2010.
60. Li Y, Xu S, Mihaylova MM, Zheng B, Hou X, Jiang B, Park O, Luo Z, Lefai E, Shyy JY, *et al*: AMPK phosphorylates and inhibits SREBP activity to attenuate hepatic steatosis and atherosclerosis in diet-induced insulin-resistant mice. Cell Metab 13: 376-388, 2011.
61. Clain DJ and Lefkowitch JH: Fatty liver disease in morbid obesity. Gastroenterol Clin North Am 16: 239-252, 1987.
62. Wang Q, Liu S, Zhai A, Zhang B and Tian G: AMPK-Mediated regulation of lipid metabolism by phosphorylation. Biol Pharm Bull 41: 985-993, 2018.